INSTITUTE OF PHYSICS PUBLISHING JOURNAL OF PHYSICS D: APPLIED PHYSICS

J. Phys. D: Appl. Phys. **40** (2007) 695–701 doi:10.1088/0022-3727/40/3/S07

Effect of a dc discharge on the supersonic rarefied air flow over a flat plate

E Menier[1], L Leger[1], E Depussay[1], V Lago[1] and G Artana[2]

[1] Laboratoire d'Aérothemique, CNRS Orléans, France
[2] Facultad de Ingeniería, Universidad de Buenos Aires, Argentina

E-mail: luc.leger@cnrs-orleans.fr

Received 30 June 2006, in final form 10 September 2006
Published 19 January 2007
Online at stacks.iop.org/JPhysD/40/695

Abstract
Recent studies have shown atmospheric plasma discharges to be an effective means of air flow control. If in subsonic conditions the plasma's effect is explained by a transfer of momentum from the charged particles to the neutral ones, in supersonic conditions it seems that the effects are mainly of thermal origin but some authors think that this effect is not the only one to act. This paper presents experimental results of stagnation pressure, spectroscopic emission and drag performed in a rarefied Mach 2 flow over a flat plate model with a half-wedge leading edge. Changes caused by a negative dc discharge located on the upper surface of the flat plate are investigated in two cases. In the first case the negative potential is applied on the upstream electrode and in the second case it is applied downstream. The second electrode is grounded. The measurements carried out indicate two opposite effects depending on the localization of the negative potential.

(Some figures in this article are in colour only in the electronic version)

1. Introduction

In recent years there has been growing interest in using weakly ionized gases for various aerodynamic applications. Indeed, weakly ionized gases appear like a new kind of flow control method when the abilities of traditional methods are subjected to natural limitations due to a strict localization and a slow response. Electroaerodynamic devices seem to be an appropriate means of increasing abilities in flow control thanks to total electric control, no moving parts and a fast response time. The electrohydrodynamic (EHD) technologies have been considered as good candidates to reduce the wave and viscous drag, heat fluxes, to produce sonic boom mitigation and to control boundary layer, turbulent transition or shock wave.

In subsonic air flows, dc discharges or dielectric barrier discharges (DBD) are used to produce 'ionic wind'. Under coulombian forces, the ions drift from the first electrode to the second one and induce a secondary flow by collisions with neutral species. This momentum is used to modify characteristics of the main air flow. The first experiments of boundary layer control were made for low velocities (up to 25 m s^{-1}) [1–6] but now efficiency is shown for flow velocities up to 75 m s^{-1} [7].

In supersonic airflows, the main problem is associated with generation of shock waves resulting in high mechanical and thermal loads on elements of an aircraft construction, sharp growth of drag force and reduction of ramjet efficiency. It has been found that gas discharge plasmas can modify the propagation of shock waves, reduce aerodynamic drag and increase lift (see, for example, Menart *et al* [8]) but the nature of the observed effects was not clear and from the very beginning there was a lot of controversial speculation around the problem [9]. Reviews of plasma applications in high speed aerodynamics are presented in [9, 10]. It appears that plasma discharges induce gas heating or non-uniform gas heating [11]. This energy addition to the flow results in an increase in the local sound speed and a reduction of gas density, that leads to expected modifications of the flow. For example, Samimy *et al* [12] proposed that the localized increase in pressure produced by the gas heating acts in a similar manner to a solid obstacle such as a tab suddenly placed in the flow. Nevertheless, some experiments have shown observations which are difficult to explain only by heat release effects. For some authors (Leonov *et al* [13], Klimov *et al* [14], Bityurin *et al* [15]), it seems that plasma generation is not equal to conventional heating because the plasma structure is self-sustained with the flow structure and the plasma influence on the flow leads to non-evident

Figure 1. The wind tunnel MARHy.

consequences. One example among these supposed non-thermal effects is the non-symmetrical effect of ac and dc discharges on the drag reduction when the polarity is changed (see Bityurin *et al* [15]). Among the advanced reasons we can find a V–T relaxation (release of stored vibrational energy) or a similar explanation as in the subsonic plasma flow control: momentum transfer due to ions accelerated by electrostatic forces ('ionic wind') [15].

In rarefied conditions, to the authors' knowledge, no work has been published in this field of research. Flow control of supersonic rarefied air flow by means of surface plasma discharge is a new topic in our laboratory. The experimental work presented here shows the measured effect of a dc discharge on a Mach 2 rarefied air flow over a flat plate. After an experimental setup presentation, pressure, spectroscopic and drag measurements will be presented and discussed.

2. Experimental setup

The experimental arrangement is made up of the following parts: the supersonic wind tunnel MARHy (Mach adaptable rarefied hypersonic), an aerodynamic flat plate, a power supply, an optical spectroscopy system and pressure and drag sensors.

2.1. Wind tunnel

The wind tunnel MARHy (figure 1) offers a wide range of Mach numbers (from 0.8 to 20) and Reynolds numbers, in a circular test section of approximately 100 mm in diameter. The rarefied air flow may be used in a continuous mode with the help of a pumping group which can pump up to $4\,\mathrm{g\,s^{-1}}$. For the present study, it operates with air and the nominal flow conditions are presented in table 1. The Mach number is equal to 2 and the mean free path is equal to 0.375 mm.

2.2. Flat plates

In these experiments, we use two flat plates. The first model under investigation is a Plexiglas flat plate with a sharp leading edge. It is 90 mm long, 80 mm wide and 4 mm thick. Two 33.5 mm-wide aluminium strips are glued onto it. The first

Table 1. Flow conditions for an 8 Pa Mach 2 nozzle.

Stagnation conditions	Flow conditions
$p_o = 63\,\mathrm{Pa}$	$P_e = 8\,\mathrm{Pa}$
$T_o = 300\,\mathrm{K}$	$T_e = 163\,\mathrm{K}$
$\rho_o = 7.44 \times 10^{-4}\,\mathrm{kg\,m^{-3}}$	$\rho_e = 1.71 \times 10^{-4}\,\mathrm{kg\,m^{-3}}$
	$V_e = 511\,\mathrm{m\,s^{-1}}$
	$Ma_e = 2$
	$\mu_e = 1.1 \times 10^{-5}\,\mathrm{Pa\,s}$
	$\lambda_e = 0.375\,\mathrm{mm}$
	$q_m = 3.34 \times 10^{-3}\,\mathrm{kg\,s^{-1}}$

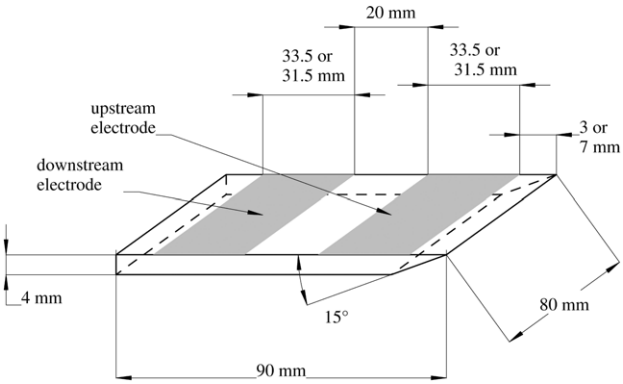

Figure 2. Schematic representation of flat plates.

electrode is placed 3 mm from the leading edge. It is 0.5 mm thick and the space between the electrodes is 20 mm. The second one is a glass flat plate with the same leading edge and the same dimensional characteristics. The two 31.5 mm width electrodes are glued in the same way but in this second case the first electrode is placed 7 mm from the leading edge. Figure 2 shows a schematic representation of the flat plates with the electrodes. In every experiment only one electrode is polarized with a negative potential and the second one is connected to the ground.

2.3. Measuring devices

2.3.1. Optical emission spectroscopy. The plasma created by the high voltage applied between the two electrodes is quite luminous as shown in figure 3. Some of its physical parameters can be determined by observing the emitted light by means of optical emission spectroscopy, which has the advantage of being a non-intrusive diagnostic tool. Rotational and vibrational spectra can be observed, and some plasma parameters, like the rotational and vibrational temperatures can be deduced. Therefore a high wavelength resolution is needed to resolve the rotational lines. The experimental setup for the measurements in the near UV and visible wavelength range is shown in figure 4.

The monochromator SOPRA F1500 of the Ebert–Fastie-type has a focal length of 1500 mm and a grating of 1800 grooves $\mathrm{mm^{-1}}$.

The plasma is imaged onto the monochromator by two plano convex lenses connected to the entrance slit by a quartz optical fibre. The detector is an intensified OMA (Princeton Instruments IRY 1024). This allows an 8.5 nm wavelength region to be scanned simultaneously. The OMA is cooled by a Peltier element, which gives an operating temperature

Figure 3. DC discharge on supersonic rarefied air flow over the flat plate.

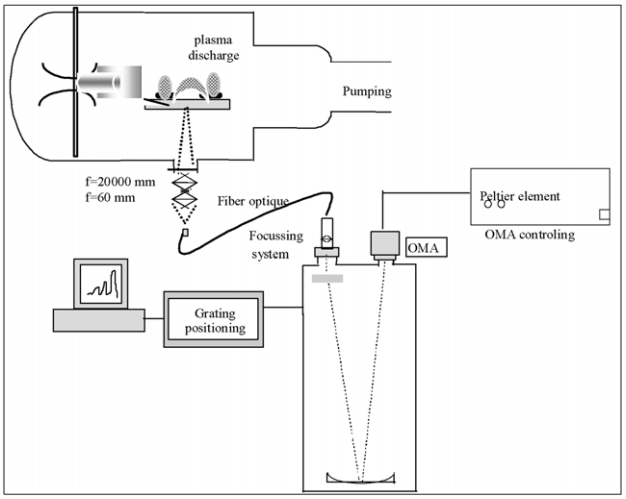

Figure 4. Optical setup.

of −35 °C. A micro-control system allows scanning of the light emitted from the cathode to the anode with a spatial resolution of 2 mm (figure 4).

The spectroscopic observation of the radiative emission, in a wavelength ranged between 200 and 900 nm, shows the preponderant emission of the second positive system of N_2 and the presence of the ion N_2^+, meaning the emission of the first negative system.

The rotational and vibrational temperatures can be determined from the first negative system of an N_2^+ spectrum. This purpose will be achieved by comparing a simulated spectrum in which the rotational and vibrational temperatures are known, with the experimental one till good agreement is obtained.

The numerical simulation calculates the direct radiative emission from the excited electronic level to the fundamental one using the equations and the rules of quantum mechanics. The excitation of the upper electronic level is done by electron impact. Decay is considered to be fully radiative. This assumption is true if the excited ions are de-excited by radiation before colliding with a molecule. If this assumption is not verified, the present calculation does not simulate the experimental spectra. This assumption can be considered if the times $t1$ between two collisions is bigger compared with the radiative decay. In our conditions $t1 = 7.7 \times 10^{-7}$ s and the radiative decay of the excited electronic level $B\Sigma$ of N_2^+ is

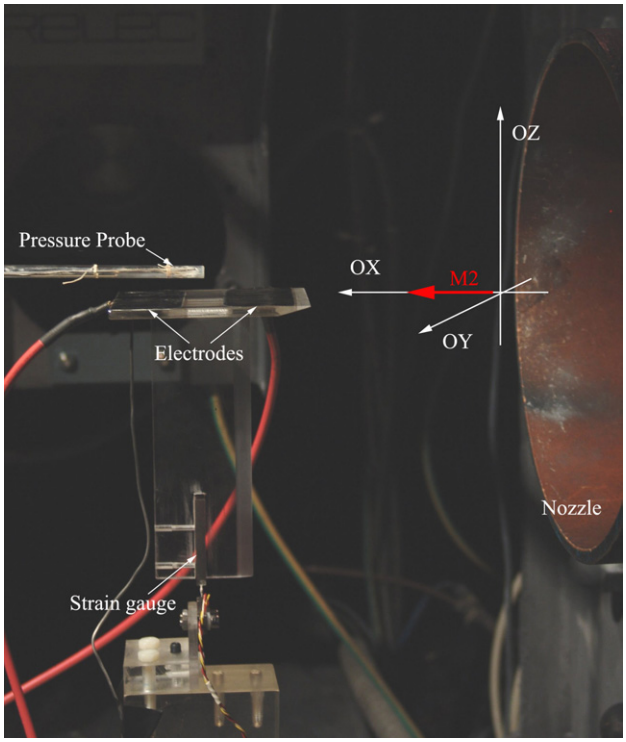

Figure 5. Photography of drag measurement setup.

$t2 = 53 \times 10^{-9}$ s, so we can consider that the de-excitation of the upper level is only due to the radiative decay.

The vibrational population of the upper level is then the result of the ground state distribution multiplied with the appropriate Franck–Condon factors. The rotational population of the upper level is considered to be identical to that of the ground state. A spectrum therefore represents the ground state rotational and vibrational distributions. The first negative system of the molecular ion of nitrogen corresponds to the transition

$$N_2^+(B\,^2\Sigma) \rightarrow N_2^+(X\,^2\Sigma).$$

A good agreement both in intensity and in the position of the spectral lines is obtained for the first negative system with vibrational and rotational constants from Krupenie [16].

2.3.2. Pressure probe and sensor. In order to avoid perturbation of the plasma by the pressure probe, this one is made of glass. It has an internal diameter of 4 mm and is 1 mm thick; such a diameter is required in low pressure conditions in order to avoid the rarefaction effects. It is therefore possible to measure the stagnation pressure inside the boundary layer in the presence of high voltage and discharge (figure 5). This probe is connected to an Mks® baratron capacitance manometer (model 626AX01TBE), which covers a range from 0 to 133 Pa (0–1 Torr) with an accuracy of 0.25% of the reading value.

2.3.3. Drag measurement. To perform the drag measurements the plates are placed on a profiled support equipped with a self-made strain gauge. This one is composed of four resistances of 350 Ω (±0.3%). As seen in figure 5, this strain

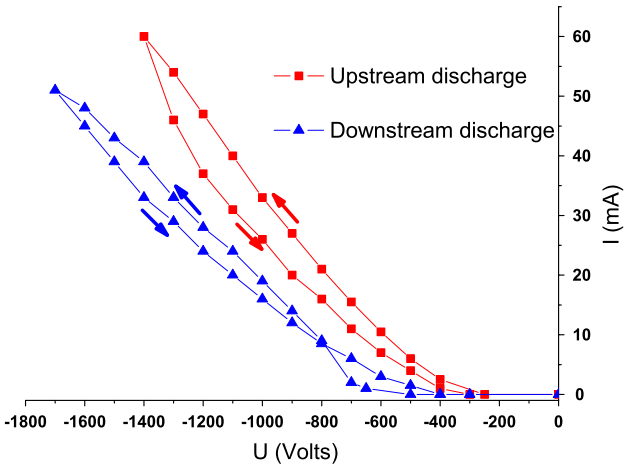

Figure 6. Current–voltage characteristic in the case of upstream discharge and downstream discharge.

gauge is situated in an area where the temperature fluctuations are about 3 °C when the discharge is on. The strain gauge is piloted by an NI-SCXI-1314 module which delivers the power supply and processes the conditioning signal.

2.3.4. Power supply and current/voltage measurement. The plasma is created by the application of a potential difference between the electrodes. Negative high voltage is created by a dc negative power supply which can deliver a potential up to −15 kV with a current up to 400 mA. A display on the power supply itself indicates the value of the applied voltage and of the mean current with an accuracy of, respectively, 10 V and 1 mA.

3. First experiment

3.1. Electrical discharge

The discharge is obtained by applying a negative dc potential either on the upstream or on the downstream electrode. The second electrode is then grounded. Figure 6 presents a typical current–voltage characteristic measured with the two types of discharges which will henceforth be called the 'downstream' and the 'upstream' discharges. As the power supply is stabilized in voltage, the measurements were obtained, first by increasing the absolute value of the voltage, then by decreasing it (let us remember that the applied voltage is negative). It can be observed that in the case of the downstream discharge it is required to apply about a 20% higher negative potential compared with the upstream case to obtain the same discharge current. This variation can be explained by the presence of a stronger density zone over the upstream electrode due to the presence of the shock wave. A hysteresis effect can be noted depending on the direction of the voltage variation.

3.2. Stagnation pressure profiles

The stagnation pressure measurements were performed in the middle of the plate in the spanwise direction, and in the middle of the inter electrode space, that is to say at a distance of 46.5 mm from the leading edge. In order to detect the influence of the discharge's presence, the measurements were

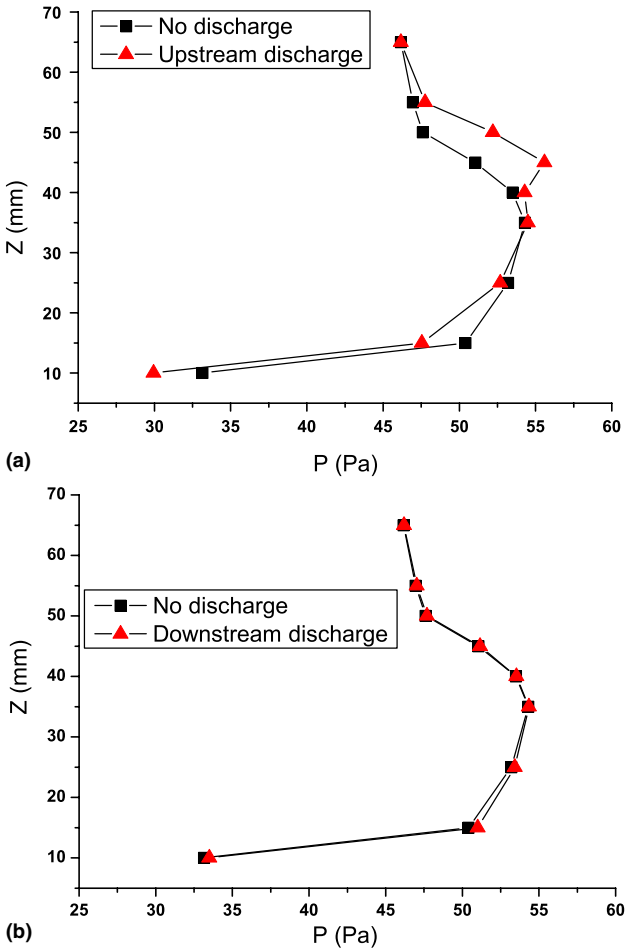

Figure 7. Pressure profile at 46.5 mm of the leading edge with and without the discharge in the case of an upstream discharge (*a*) and a downstream discharge (*b*). $U = -1$ kV, $I = 30$ mA for the upstream discharge; $U = -1.2$ kV, $I = 25$ mA for the downstream discharge.

realized with the discharge on and off. Moreover, if the discharge is on, the fact that the active electrode is upstream or downstream is also studied. Particular attention was paid to maintain the electrical power constant equal to 30 W for all the experiments presented. The discharge characteristics for the upstream configuration are −1 kV and 30 mA. Regarding figure 6, it is seen that the downstream configuration needs a higher applied voltage, −1.2 V and a smaller current, 25 mA, to keep the electrical power constant. A measurement protocol was established taking into account the different delays needed to reach the different equilibrium effects like the aerodynamic and thermal effects on the pressure probe and the temperature of the flat plate. An infra red camera allows controlling the flat plate temperature. The stagnation pressure profiles are presented in figure 7.

Figure 7(*a*) shows the comparison of the stagnation pressure profiles with the upstream discharge and without the discharge. It can be observed that the presence of the discharge induces a decrease in the pressure inside the boundary layer. This decrease can be observed up to 25 mm from the plate surface. We can see that the stagnation pressure profile is shifted from about 3 Pa at 15 mm from the wall, which represents a reduction of 6% of the stagnation pressure. At 40 mm from the wall, without discharge, the stagnation

Table 2. Spectroscopic results over the active electrode in the cases of upstream and downstream discharges.

Downstream discharge -1 kV, 19 mA	Tr = 230 K, Tv = Te = 1100 K
Upstream discharge -1 kV, 30 mA	Tr = 230 K, Tv = Te = 1100 K

pressure decreases quickly. It goes from about 52 to 46 Pa in 10 mm. This is due to the fact that the pressure probe meets the oblique shock wave created by the leading edge. We can see that when the discharge is applied this decrease appears slightly further, about 5 mm, from the wall. It thus seems that the discharge induces an effect on the shock wave. In the first approach, by considering that the shock is 5 mm further from the wall when the discharge is applied, the profile is measured at 46.5 mm from the leading edge and one obtains an increase in the shock wave angle of approximately 4°.

It seems that this effect is essentially due to heating. A heating of the boundary layer as well as the plate surface, induces an increase in the viscosity, leading to an increase in the speed of sound, and changing the flow configuration (see for example [10]). This assumption was confirmed by numerical simulation by a direct simulation Monte Carlo method (to be published).

The case of the downstream discharge is presented in figure 7(*b*). As can be observed, the presence of the discharge does not seem to have an effect on the stagnation pressure profile. Nevertheless, one can observe a light increase in the pressure at 15 mm from the plate surface. This very weak difference is repetitive and was observed in other experiments.

If the effects were due to thermal heating, one could expect, as the power of the discharges are similar, that the effect would be the same or slightly smaller for the downstream case due to the position of the pressure probe compared with the active electrode. What seems to be an opposite effect appears more difficult to justify.

So as to characterize the thermodynamic state of the gas in the presence of the discharge and to observe if the discharge is equivalent in both cases, temperature measurements by spectroscopic analysis were made.

3.3. Temperature measurements by spectroscopic analysis

Optical measurements have been realized over each active electrode, under two similar electrical configurations. The rotational and vibrational temperatures have been determined by analysing the N_2^+ negative system spectra using the comparison method. The temperatures are obtained with a precision of 10 K. The results are presented in table 2. The rotational and vibrational temperatures are found to be the same in both cases.

An example of comparison between a simulated and an experimental spectrum is presented in figure 8. The experimental spectrum presented was obtained over the active electrode polarized at -1 kV in the downstream case.

4. Second experiment

For the second experiment we wished to use more powerful discharges, and to avoid damage to the plate due to heating,

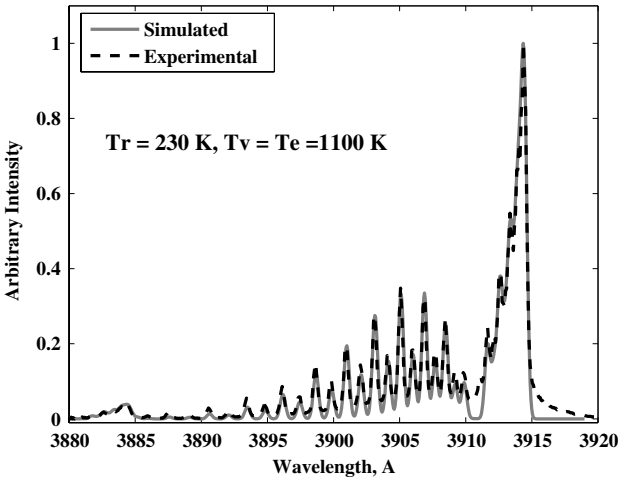

Figure 8. Comparison between an experimental and a calculated spectra of N_2^+ in the case of a downstream discharge, $U = -1$ kV, $I = 19$ mA.

a glass plate was used. This material is indeed more resistant and is not likely to become deformed during experiments.

4.1. Pressure measurements

Here we present the evolution of the pressure as a function of time. The duration of the recording is approximately 20 min. During this time the discharge is applied and then turned off. The pressure probe is placed 15 mm from the plate and 48.5 mm from the leading edge for all measurements presented here. Figure 9 shows the stagnation pressure evolution as a function of time when the upstream discharge is applied for about 150 s. For this experiment the potential is -1.67 kV and the discharge current is then 55 mA; thus the power is about 91 W. We can see that as soon as the discharge is turned on the stagnation pressure decreases quickly. This confirms the measurements previously carried out. When the discharge is turned off, it is noticeable that the pressure returns slowly to the initial value. This behaviour shows that there is a thermal effect.

Figure 9 shows the stagnation pressure evolution as a function of time when we applied the downstream discharge about the same time as that in the preceding experiment. For this experiment the applied potential is -1.76 kV and the discharge current is 58 mA; thus the power used is about 100 W. We can see that when the discharge is applied the stagnation pressure increases. This experiment confirms our first observations. This increase remains weak, as observed previously in spite of the increase in the discharge power. Also, the change in pressure is low compared with the case of the upstream discharge. When the discharge is turned off, the stagnation pressure decreases and returns to its initial value much more quickly. This return to the initial value does not occur in the same way. If this effect was only due to heat release, the behaviour in time of the pressure when the discharge is switched off should happen in a way similar to the case of the upstream discharge.

4.2. Drag measurements

The drag measurements were carried out at the same time as the pressure measurements, using a strain gauge placed on